Does convective aggregation need to be represented in cumulus parameterizations?

Isabelle Tobin,[1] Sandrine Bony,[1] Chris E. Holloway,[2] Jean-Yves Grandpeix,[1] Geneviève Sèze,[1] David Coppin,[1] Steve J. Woolnough,[2] and Rémy Roca[3]

Received 1 February 2013; revised 2 July 2013; accepted 20 August 2013; published 2 October 2013.

[1] Tropical deep convection exhibits a variety of levels of aggregation over a wide range of scales. Based on a multisatellite analysis, the present study shows at mesoscale that different levels of aggregation are statistically associated with differing large-scale atmospheric states, despite similar convective intensity and large-scale forcings. The more aggregated the convection, the dryer and less cloudy the atmosphere, the stronger the outgoing longwave radiation, and the lower the planetary albedo. This suggests that mesoscale convective aggregation has the potential to affect couplings between moisture and convection and between convection, radiation, and large-scale ascent. In so doing, aggregation may play a role in phenomena such as "hot spots" or the Madden-Julian Oscillation. These findings support the need for the representation of mesoscale organization in cumulus parameterizations; most parameterizations used in current climate models lack any such representation. The ability of a cloud system-resolving model to reproduce observed relationships suggests that such models may be useful to guide attempts at parameterizations of convective aggregation.

Citation: Tobin, I., S. Bony, C. E. Holloway, J. Y. Grandpeix, G. Sèze, D. Coppin, S. J. Woolnough, and R. Roca (2013), Does convective aggregation need to be represented in cumulus parameterizations? *J. Adv. Model. Earth Syst.*, *5*, 692–703, doi:10.1002/jame.20047.

1. Introduction

[2] Through its strong interactions with atmospheric thermodynamics, cloudiness, and large-scale circulations, deep moist convection plays a key role in the energy and water transfers within the climate system. Consistently, its representation in general circulation models crucially controls the simulation of climate, its variability, and change.

[3] Since convective processes operate at a scale which is smaller than the resolution of current climate models, their representation requires the use of parameterizations. Several cumulus parameterizations have thus been developed to predict, based on the resolved large-scale variables, the collective effects of an ensemble of cumulus on the large-scale atmosphere (see *Arakawa* [2004] for a review). However, parameterizations inherently constitute a simplistic representation and, despite modeling efforts over the last decades, capturing all aspects of the convection-large-scale atmosphere coupling through parameterizations remains a challenge. One reason is that the key aspects are presumably not all well known, but even the well-identified aspects of this interaction, such as the sensitivity of convection to tropospheric humidity, are still difficult to represent [e.g., *Derbyshire et al.*, 2004; *Del Genio*, 2012]. Cumulus parameterization shortcomings are considered to be responsible for some of the difficulties experienced by climate models, such as deficiencies in the simulation of intraseasonal variability, including the Madden-Julian Oscillation (MJO) [e.g., *Lin et al.*, 2006; *Thayer-Calder and Randall*, 2009; *Kim et al.*, 2011], or the tendency of models to rain too lightly and too steadily [*Stephens et al.*, 2010]. They also likely contribute to the uncertainty in climate sensitivity [*Sanderson et al.*, 2010].

[4] Global climate simulations using cloud resolving models are still at their infancy, owing to their computational cost. In recent years, superparameterizations [*Khairoutdinov and Randall*, 2001] have been developed as a way to partly get round these issues. Despite promising results [e.g., *Thayer-Calder and Randall*, 2009; *Zhu et al.*, 2009], this technique has its own difficulties and is still computationally demanding. For this reason and because the development of cumulus parameterizations is also a way to encapsulate our knowledge and understanding of convective processes, it remains imperative to improve convection schemes.

[5] In most cumulus parameterizations, a set of assumptions and parameters is used to represent processes, such as entrainment and detrainment rates,

[1]Laboratoire de Météorologie Dynamique, CNRS, University of Pierre and Marie Curie (UPMC), Paris, France.
[2]Department of Meteorology, NCAS-Climate, University of Reading, Reading, United Kingdom.
[3]Laboratoire d'Etudes en Géophysique et Océanographie Spatiales, National Center of Spatial Studies (CNES), Toulouse, France.

Corresponding author: I. Tobin, Laboratoire de Météorologie Dynamique, CNRS, UPMC, Paris, France. (isabelle.tobin@lmd.jussieu.fr)

1942-2466/13/10.1002/jame.20047

precipitation efficiency, or rain evaporation, which tightly specifies the statistical interactions of an ensemble of convective clouds with its large-scale environment. In nature, however, moist convection exhibits a variety of forms of mesoscale organization, ranging from isolated convective cells a few kilometers across to multicellular thunderstorms to organized mesoscale convective systems, such as squall lines and mesoscale convective complexes [e.g., *Redelsperger*, 1997; *Laing and Fritsch*, 1997; *Houze*, 2004]. Recent cloud-system resolving model (CSRM) studies, carried out in a radiative-convective equilibrium framework (RCE), have also simulated multiple equilibria characterized by different degrees of convective organization [e.g., *Bretherton et al.*, 2005; *Khairoutdinov and Emanuel*, 2010; *Muller and Held*, 2012]. The question remains open whether these various types and degrees of convective organization are associated with differences in the ways that convection interacts with the large-scale atmosphere and whether these differences may be captured by current cumulus parameterizations.

[6] Many studies have highlighted that interactions between organized convection and the large-scale atmosphere differ from those associated with ordinary convection by pointing out, among other factors, the shear generation of kinetic energy by distinctive momentum transport of organized convection [*Wu and Moncrieff*, 1996; *Moncrieff and Klinker*, 1997] or the role of mesoscale circulations and of the heating profiles associated with anvils and rain evaporation [*Houze*, 2004]. Consistently, several studies have proposed ways to represent features related to convective organization: *Wu and Moncrieff* [1996] outlined a dynamical model of organized convection coupled to a mass-flux-based parameterization to calculate the momentum-related effects, *Donner* [1993] included mesoscale effects of anvils in his cumulus parameterization, *Grandpeix and Lafore* [2010] developed a parameterization of density currents associated with organized convection, and *Mapes and Neale* [2011] used a prognostic variable "org" to take into account forcings related to any organizational feature. Although these efforts have resulted in some model improvements [e.g., *Rio et al.*, 2009; *Mapes and Neale*, 2011], the exploration of features of convective organization that may play an active role in the convection-large-scale atmosphere interactions and in the performance of climate models deserves further investigation.

[7] At larger (synoptic) scales, cloud-system resolving model studies have highlighted that, despite similar rain rates and large-scale forcings, different convective aggregation states were associated with different mean atmospheric states [e.g., *Bretherton et al.*, 2005; *Muller and Held*, 2012]. These results have been confirmed by a recent observational study [*Tobin et al.*, 2012]. Such synoptic relationships can be partially captured by general circulation models (GCMs) since the gridbox size allows for a partial resolution of the large-scale convective organization. The question arises, however, whether there are relationships between the aggregation state of convection and the large-scale atmosphere at the scale of a typical GCM gridbox, i.e., at a scale where the effects related to mesoscale convective organization are likely missing from GCMs? This question provides the motivation for the present study.

[8] Section 2 presents an observational analysis of relationships between mesoscale convective aggregation and the large-scale atmospheric state. Section 3 explores these relationships in a cloud-system resolving model framework. Then, section 4 discusses the implications of our findings for climate and cumulus parameterizations.

2. Observational Study

2.1. Methodology

[9] Statistical relationships between the large-scale atmosphere and the aggregation state of deep convection are investigated in observations over domain sizes typical of a current climate model gridbox. For this purpose, we use the methodology developed by *Tobin et al.* [2012, hereafter T12], which consists of compositing large-scale atmospheric variables by the degree of aggregation of convection. This latter is characterized by a combined measure of the number of convective clusters N and the clumping of clusters D_0 within a given domain (see T12). Here, only the number N is used because it is straightforward to interpret: low Ns characterize aggregated convection (Figure 1a) while high Ns indicate loose (or "pop corn") organization (Figure 1b). A priori, N is not sufficient to quantify the degree of convective aggregation since numerous clusters (high N) can be considered as aggregated convection if they are clumped. However, it has been shown in T12 and confirmed in the present study that N is statistically sufficient to discriminate between the different degrees of aggregation. This is because the clusters are well distributed over the domain in most cases (see T12). For the purpose of the study, computations of N and large-scale variables are made over $3^\circ \times 3^\circ$ domains (Figure 1), instead of $10^\circ \times 10^\circ$ as in T12. To ensure that differences among the aggregation classes are not driven by differences in deep convective intensity within the domains or by differing large-scale forcings, the composites are computed for a given convective intensity, a given Sea Surface Temperature (SST) and comparable large-scale dynamical conditions. The proxy used for the amount of convection is the domain-averaged instantaneous precipitation rate. In addition, domains are selected such as to avoid substantial differences in the total convective area (defined as the sum of the convective clusters areas). Large-scale vertical velocity at 800, 500, and 300 hPa levels is used as a proxy for large-scale dynamics. The large-scale variables analyzed in this study are atmospheric humidity, cloudiness, longwave radiative fluxes at the surface and at the top of the atmosphere (TOA) and shortwave radiation at the TOA.

2.2. Data

[10] The number of clusters N is computed from the infrared (10–12.5 μm) brightness temperature (Tb), measured every 30 min by the European geostationary

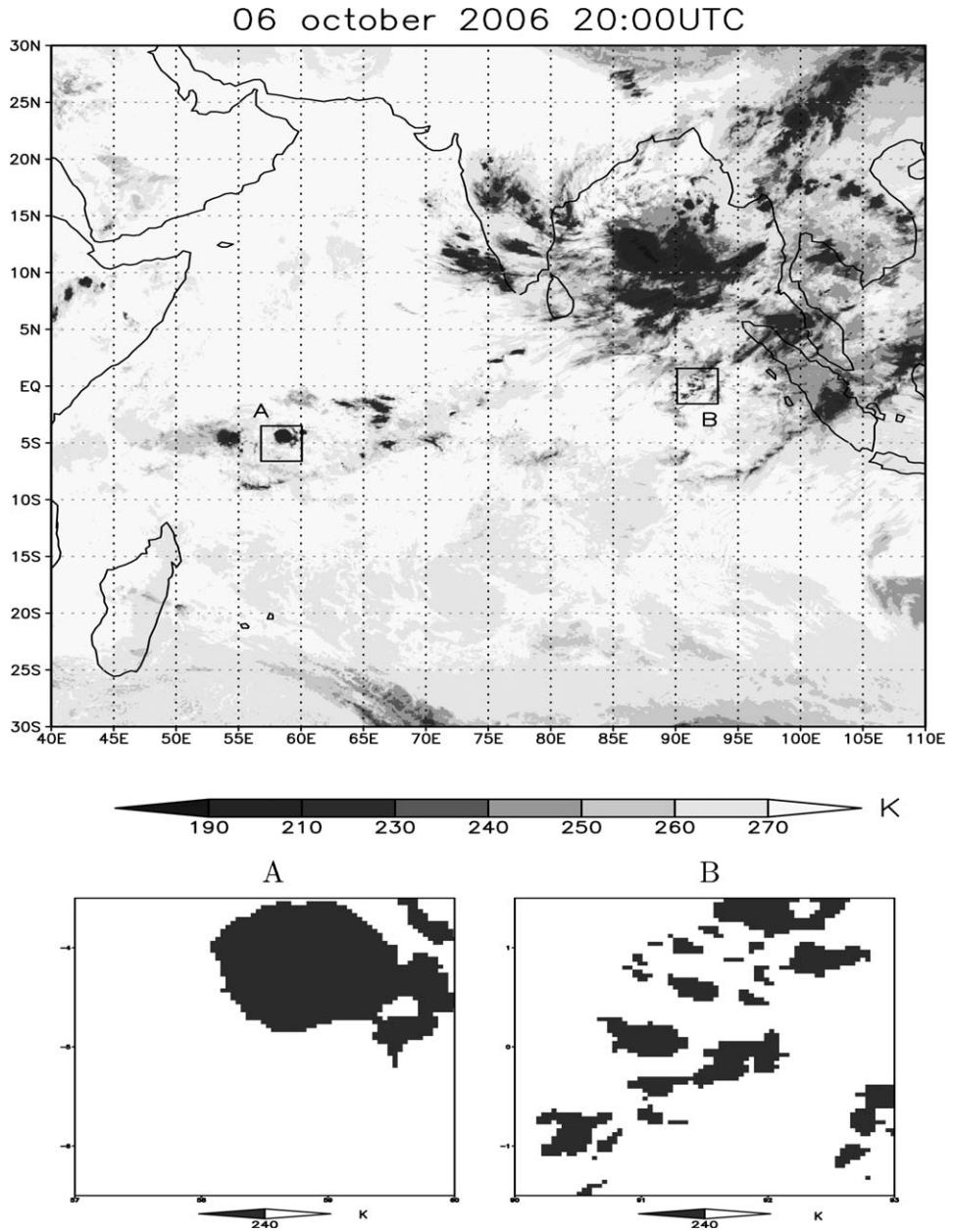

Figure 1. Top: Snapshot of Meteosat-5 infrared brightness temperature (Tb) on the 6 October 2006 at 20:00 UTC. The two black squares are examples of the $3^\circ \times 3^\circ$ domains under consideration in this study. Bottom: Segmentation of the domains A and B into deep convective regions ($Tb < 240$ K) and deep convective-free environment ($Tb > 240$ K). Domain A is characterized by a total convective area of 20% and two convective clusters and domain B by a total convective area of 16% and 28 convective clusters.

satellite Meteosat 5, at a 5 km spatial resolution at nadir. As in T12, a convective cluster is defined as an area made up of adjacent pixels whose Tb is colder than a threshold of 240 K. Pixels warmer than this threshold are considered as belonging to the environment of deep convection (Figure 1). Pixels are considered adjacent either if they share one side (so-called "four connectivity") or one side or a corner (so called "cross connectivity"). Here, the four-connectivity is used as in T12 but our results are not sensitive to this choice. The 240 K threshold value has been chosen in order to locate convective regions as a whole (i.e., core and parts of anvils) and not only convective cells (see T12). However, sensitivity tests to this value have been conducted up to 220 K, which lead to similar results. Note that the Meteosat Tb dataset resolution is much finer than the 50 km Tb dataset used in T12 (which was focusing on the synoptic scale), as required to discriminate between the different degrees of mesoscale convective aggregation over a domain size of $3^\circ \times 3^\circ$.

[11] The products RAIN, ASST, PRW, and FNET from the $1^\circ \times 1^\circ$ twice-daily Hamburg Ocean

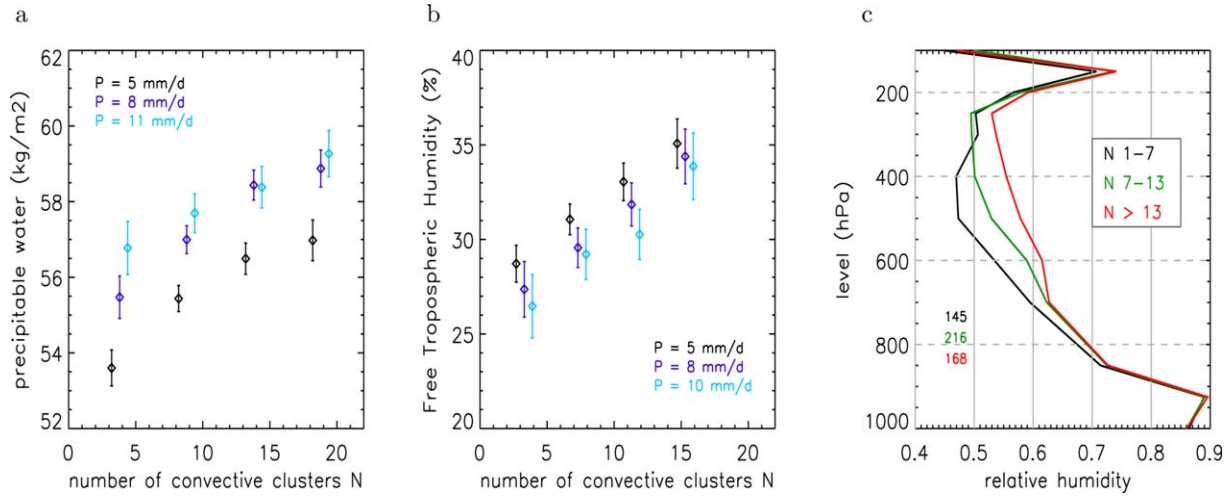

Figure 2. (a) Domain-averaged precipitable water composited by the number of clusters N for three regimes of precipitation above the Indian Ocean (P1: 5 mm d^{-1}; P2: 8 mm d^{-1}; P3: 10 mm d^{-1}). (b) Same as (a) but for free tropospheric humidity. (c) Domain-averaged AIRS relative humidity profiles composited by N for a precipitation rate of 8 mm/d (P2) and a total convective area of about 20%. In (a), (b), and (c), for each precipitation regime, SST, and the instantaneous vertical-velocity profiles are comparable among the N classes (the SST is around 28°C and the vertical velocities at 800, 500, and 300 hPa are, respectively, for P1: about −45 hPa d^{-1}, −25 hPa d^{-1}, and −20 hPa d^{-1}; for P2: about −60 hPa d^{-1}, −45 hPa d^{-1}, and −40 hPa d^{-1}; for P3: about −70 hPa d^{-1}, −50 hPa d^{-1}, and −40 hPa d^{-1}). The error bars in (a) and (b) correspond to $\pm\frac{2\sigma}{\sqrt{n}}$ (σ is the standard deviation; n is the sample size). Note that the FTH and AIRS products are both derived from infrared measurements, and are thus "clear-sky biased." Notable differences, however, are found in the absolute values, which probably stem from differing "cloud-clearing" methods [*Susskind et al.*, 2003; *Brogniez et al.*, 2006].

Atmosphere Parameters and Fluxes from Satellite Data (HOAPS-3) archive [*Andersson et al.*, 2010] are used to compute domain averages of the precipitation rate, SST, precipitable water and the net longwave radiative fluxes at the surface, respectively. Relative humidity is analyzed with the twice-daily 1° × 1° data product derived from the Atmospheric InfraRed Sounder (AIRS) on board the Aqua satellite [*Aumann et al.*, 2003], and from the FTH product (Free Tropospheric Humidity; *Brogniez et al.* [2004, 2006] derived from Meteosat water vapor radiances (6.2 μm channel) at a 0.625° resolution, 3-hourly. The large-scale dynamics is characterized by the large-scale vertical velocity from ERA-interim reanalyses produced by the European Center for Medium-Range Weather Forecast (ECMWF) [*Simmons et al.*, 2007]. Outgoing longwave radiation (OLR) is derived either from the daily interpolated National Oceanic and Atmospheric Administration (NOAA) OLR at 2.5° resolution [*Liebmann and Smith*, 1996] or calculated from both Meteosat infrared (IR) and water vapor (WV) channels (5 km resolution at nadir, every 30 min), using the multilinear regression established by *Roca et al.* [2002] (equation (1).)

$$\mathrm{OLR} = a_0 + a_1 L_{\mathrm{IR}} + a_2 L_{\mathrm{IR}}^3 + a_3 L_{\mathrm{IR}} / \cos(\theta) + a_4 L_{\mathrm{WV}} + a_5 L_{\mathrm{WV}}^2 \quad (1)$$

where L_{IR} and L_{WV} are the Meteosat IR and WV radiances, θ is the zenithal viewing angle of Meteosat, and the values of the regression coefficients are, respectively, 65.48, 14.19, −0.0079, 1.841, 61.33, and −11.03.

[12] The OLR derived from the 3-hourly 2.5° × 2.5° International Satellite Cloud Climatology Project (ISCCP) FD TOA product [*Zhang et al.*, 2004] is also analyzed. The radiative cooling of the atmospheric column is then estimated by subtracting FNET from the OLR products. Cloudiness is characterized by the cloud optical thickness and cloud-top pressure derived from the 3-hourly 30 km ISCCP DX products [*Rossow and Schiffer*, 1999]. The shortwave radiative fluxes at the TOA, from which the planetary albedo is inferred, are derived from ISCCP FD TOA data.

[13] The analysis presented in this paper is carried out above the tropical Indian Ocean (40°E-100°E/30°S-30°N) during the July 1998–December 2005 period, which corresponds to the overlapping period between the HOAPS archive and the datasets derived from Meteosat 5, then positioned over 0°N-63°E. The analysis has also been conducted over the Atlantic Ocean for the 1990–1999 period, and led to similar findings (not shown). Except for the analysis of OLR-NOAA daily dataset, the analysis is conducted at the instantaneous scale.

2.3. Results

[14] The compositing analysis shows that for a given domain-averaged precipitation rate, given SST and large-scale dynamics, the mean atmospheric humidity varies with the degree of aggregation of convection (Figure 2): the more aggregated the convection is (the

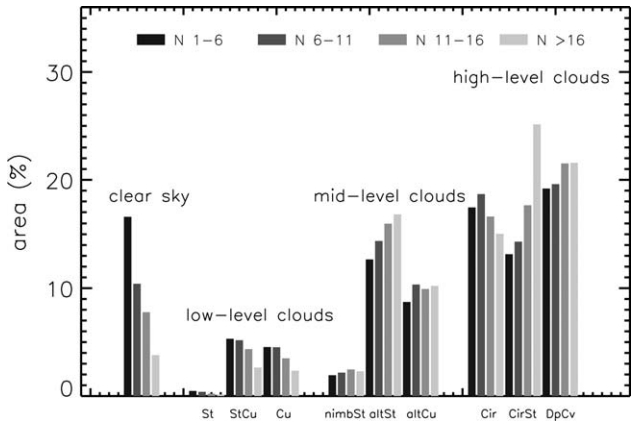

Figure 3. ISCCP cloud classification composited by N for a precipitation rate of 8 mm/d and a total convective area of about 20%. The cloud types are from left to right stratus (St), stratocumulus (StCu), cumulus (Cu), nimbostratus (nimbSt), altostratus (altSt), altocumulus (altCu), cirrus (Cir), cirrostratus (CirSt) and deep convective clouds (DpCv). SST and the instantaneous vertical-velocity profiles are comparable among the N classes.

lower N), the drier the atmosphere is. Precipitable water differences of about 3–4 kg m^{-2} are observed between the least and the most aggregated classes (Figure 2a). Relative humidity (RH) profiles show consistent results and point out that humidity differences stem primarily from the mid and upper troposphere: while relative humidity profiles do not differ much among aggregation classes up to 800 hPa, the free troposphere exhibits differences of about 0.1, which are maximum around 400–500 hPa (Figure 2c). The analysis of FTH confirms these findings (Figure 2b). Therefore, convective aggregation and atmospheric humidity are not only anticorrelated at the synoptic scale (T12) but also at the mesoscale.

[15] To investigate whether these humidity differences between aggregation states are associated with differences in cloudiness, we analyze the daytime cloud classification established by ISCCP using the cloud optical thickness and the cloud-top pressure [*Rossow and Schiffer*, 1999] (Figure 3). As expected, aggregated situations appear to be characterized by a reduced cloud amount in the environment. The clear-sky area of the domain increases from a few percent for the least aggregated state to over 15% for the most aggregated state. Despite the lower reliability of the ISCCP classification in the case of overlapping cloud layers, it clearly appears that this cloud amount reduction with increasing aggregation mostly stems from the reduction of the altostratus and cirrostratus cloud amounts.

[16] Differences in humidity and cloudiness are expected to affect longwave radiation. Indeed, the compositing analysis of longwave fluxes reveals that the tropospheric radiative cooling increases by 20–30 W m^{-2} from the least to the most aggregated states, due to the enhanced longwave radiation escaping to space (OLR) when convection is more aggregated (Figure 4a and 4b) (the net longwave radiative fluxes at the surface do not differ among the aggregation classes). Both Meteosat and OLR-NOAA datasets (Figures 4a and 4b), along with ISCCP FD OLR dataset (not shown), lead to the same findings qualitatively and quantitatively. Therefore, at the mesoscale, as found at the synoptic scale (T12), convective aggregation is positively correlated with OLR and atmospheric radiative cooling.

[17] The reflected shortwave radiative fluxes at TOA are also likely to be affected by differences in cloudiness. This is examined by compositing the planetary albedo by N. The planetary albedo is defined as the ratio of outgoing shortwave radiation to incoming

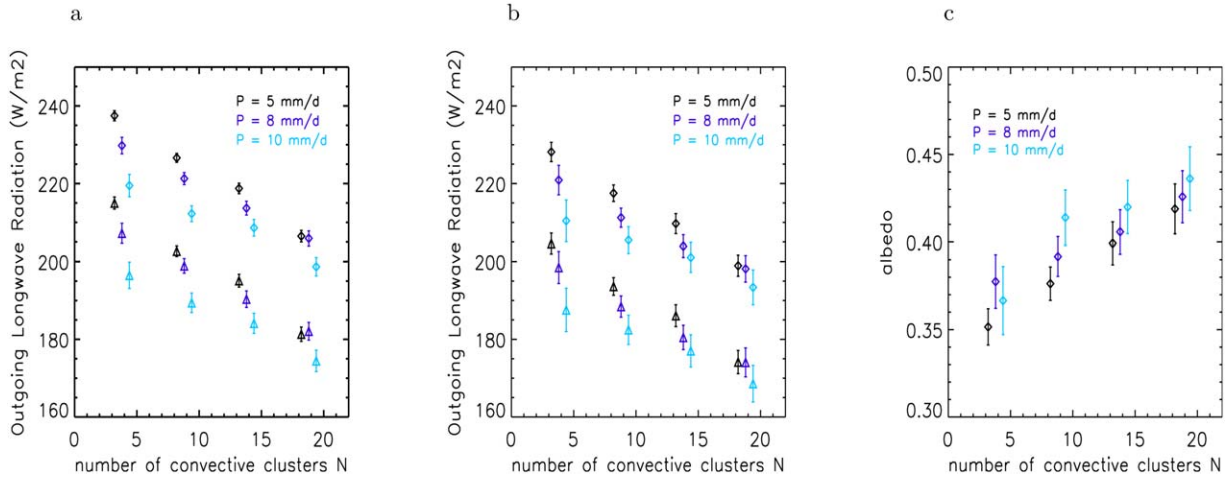

Figure 4. (a)-(b) Domain-averaged outgoing longwave radiation (OLR) (diamonds) and radiative cooling (triangles) composited by the number of clusters N for three different amounts of convection above the Indian Ocean, over the 1998–2005 period. (a) calculated OLR from Meteosat (b) daily OLR from NOAA. (c) Same as (a) for domain-averaged planetary albedo. For each convective intensity regime, SST and the instantaneous vertical-velocity profiles are comparable among the N classes.

shortwave radiation. Investigating the albedo instead of the reflected shortwave flux enables us to avoid differences in the latter resulting from differences in the incoming solar flux among the N classes. The planetary albedo is shown to decrease with aggregation, exhibiting a 0.05 difference between the least to the most aggregated convective states (Figure 4c). Thus, aggregated situations absorb more solar energy than scattered convective situations. The magnitude of the absorbed solar energy difference will depend on the amount of incoming solar radiation, this difference being maximum in the summer warmer season at the maximum insolation time of the day, and being null during nighttime. On average over days, seasons, and years, however, the tropical insolation being about 400 W m^{-2}, a 0.05 albedo difference leads to a 20 W m^{-2} difference in reflected shortwave flux between the least and the most aggregated states examined here.

[18] Therefore, as found in T12, shortwave effects largely offset longwave effects at TOA, which results in a weak sensitivity of the Earth's radiation budget to the degree of convective aggregation. However, since the atmosphere is much more transparent to shortwave radiation than to longwave radiation, differences in the shortwave and longwave components are necessarily associated with differing vertical redistributions of energy between the least and the most aggregated states. It is likely to affect the surface and atmosphere energy budgets.

[19] A comprehensive budget analysis, however, requires the investigation of surface turbulent heat fluxes: unlike at the synoptic scale (T12), turbulent fluxes do not exhibit any robust sensitivity to the aggregation state of convection (not shown). As a result, the sensitivity of the surface energy budget to convective aggregation is controlled by differences in shortwave fluxes (since the net longwave radiative fluxes at the surface are not sensitive to the aggregation state) while the sensitivity of the net diabatic heating within the atmosphere is dominated by the longwave fluxes difference. Therefore, the surface gains more energy (by up to ~20 W m^{-2}) and the atmosphere loses more energy (by up to 20–30 W m^{-2}) in situations of aggregated convection than in situations of scattered convection.

3. Cloud-System Resolving Model Analysis

[20] Cloud-system resolving models (CSRM) constitute potential tools for understanding the mechanisms underlying the observed relationships, provided that they are able to reproduce them. Here, we compare the above observational results with analysis results derived from the United Kingdom (UK) Met Office Unified Model (UM).

3.1. Model Data and Methodology

[21] The CSRM simulation analyzed here is a 10 day-case study (9–15 April 2009) over a large tropical domain (~20°S-20°N and 42°E-180°E). This case corresponds to an active phase of the Madden-Julian Oscillation (MJO). This simulation is part of "Cascade," a UK consortium project aiming at better understanding the organization of tropical convection on a wide range of scales. Further details related to this project, the UM and this particular simulation (referred to as "4 km 3Dsmag") can be found in *Holloway et al.* [2012]. The spatial resolution is 4 km, which allows for resolving only the basic cumulonimbus structure. The outputs are available every hour. Since the IR brightness temperature (Tb) is not a model output variable, the OLR variable is used to detect deep convective situations and to compute N. At the spatial and temporal resolutions of the model, the OLR signal comes primarily from the top of clouds, which behaves like a blackbody to first approximation. Thus, the correspondence between Tb and OLR can be assessed through the Stefan-Boltzmann law characterizing blackbody radiation: $\mathrm{OLR} \simeq \sigma Tb^4$ where $\sigma = 5.67 \cdot 10^{-8} \mathrm{Wm^{-2}K^{-4}}$. The OLR threshold corresponding to a Tb threshold of 240 K is about 190 W m^{-2}.

[22] Note that the quantitative comparison between observations and model results is not straightforward since the parameter N is calculated from 4 km gridboxes in one case and from 5 km pixels in the other case, which results in a different number of pixels within the delimited 300 km domains.

3.2. Results

[23] The compositing analysis shows that the CSRM reasonably reproduces the relationships between the aggregation state of convection, atmospheric humidity, and radiation observed at the mesoscale: when convection is more aggregated, the free troposphere is drier (by about 10%) (Figure 5a), the atmospheric radiative cooling is stronger by about 20 W m^{-2} due to an enhanced OLR (Figure 5b), and the planetary albedo is lower by about 0.05–0.07 (Figure 5c). An analysis of the liquid and ice water content predicted outside deep convective regions reveals that aggregated situations are associated with less condensate in the environment both in terms of amount and spatial extent, especially the ice condensate. This is qualitatively consistent with the observed reduction of upper level cloud amount. Like in observations, the surface turbulent fluxes do not exhibit any significant sensitivity to the aggregation state of convection (not shown). Note, however, that significant differences are found between the CSRM-simulated and observed mean state: the simulated mean OLR, albedo, and upper troposphere humidity are, respectively, 0.15 lower, 20–30 W m^{-2} higher, and 0.10–0.20 lower than in observations. There are several potential reasons for these biases. First, the observational analysis time period is much longer than the simulation time period, so it is difficult to make statements about the model bias based on these results. However, the 4 km 3Dsmag model does have an overall high OLR bias and dry tropospheric humidity bias compared with observations over the same period (see *Holloway et al.* [2013], their Figure 2 and Supporting Information, Figure S1). These biases likely reflect limitations on the ability of a 4 km explicit convection model to resolve the full range of cloud processes,

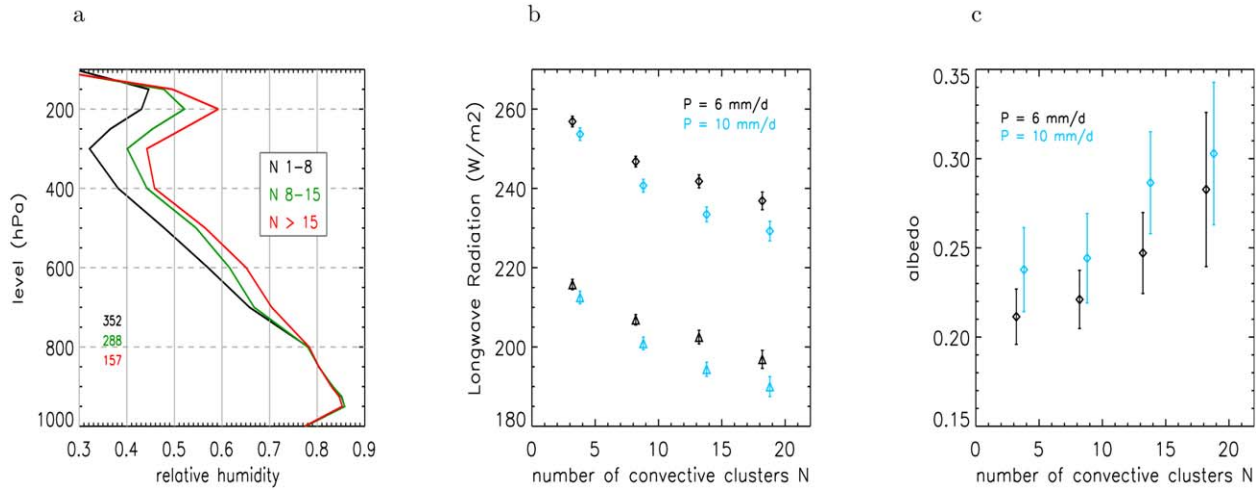

Figure 5. Cloud-system resolving model *N*-composite analysis. (a) Domain-averaged relative humidity profiles composited by the number of clusters *N* for a precipitation rate of 10mm/d and a total convective area of about 20%. (b) Domain-averaged outgoing longwave radiation (OLR) (diamonds) and tropospheric radiative cooling (triangles) in W m^{-2} composited by *N* for two different convective activities (domain-averaged precipitation rate of 6 mm/d and total convective area of about 15%; precipitation rate of 10 mm/d and total convective area of about 20%). (c) Same as (b) but for domain-averaged planetary albedo. For each convective intensity regime, SST and the instantaneous vertical velocity profiles are comparable among the *N* classes.

including shallow convection and mixing at cloud edges. Furthermore, there are likely to be deficiencies in the ability of subgrid scale parameterizations, such as microphysics and subgrid mixing schemes, to represent subgrid processes. These models have also not been tuned to accurately simulate climatological large-scale radiation fluxes in the way that most global models have been tuned.

4. Conclusions, Discussion, and Implications

4.1. Summary

[24] The observational analysis presented in this paper has highlighted over tropical oceans the existence, at the scale typical of a climate model gridbox, of various degrees of convective aggregation for a given convective activity and large-scale forcings. Furthermore, these different aggregation states are statistically associated with different large-scale atmospheric states. Situations where convection is more aggregated are characterized by a drier free troposphere and a larger fractional clear sky region, due to reduced mid and high-level cloudiness. As a result, longwave radiation escaping to space is enhanced, which leads to a stronger tropospheric radiative cooling on average over the domain. Consistently with the reduced cloudiness, the planetary albedo and the reflected shortwave radiation are lower. Surface turbulent fluxes, however, do not exhibit any significant sensitivity to convective aggregation.

[25] These results show that:

[26] Despite a strong sensitivity of longwave and shortwave radiative fluxes at TOA, on daily to interannual timescales, the Earth's budget is not significantly affected by the aggregation state of convection because of a near cancellation between the shortwave and longwave anomalies.

[27] On the other hand, the surface gains more energy and the atmosphere diabatically losses more energy when convection is more aggregated.

4.2. Consistency With Numerical Results and Previous Studies

[28] Additionally, this work shows that the UK Met Office UM at CRSM resolution over a large domain reasonably reproduces the observed relationships. This gives confidence in the performance of such models to treat convection-large-scale atmosphere interactions and increases the robustness of the observational results.

[29] This mesoscale study presents several findings that are consistent with previous studies, both numerical (RCE framework, [e.g., *Bretherton et al.*, 2005; *Khairoutdinov and Emanuel*, 2010; *Muller and Held*, 2012]) and observational (T12), including the fact that on larger scales, for given overall convective intensity and large-scale forcings, deep convection exhibits multiple levels of aggregation which are characterized by different large-scale atmospheric states. For instance, at particular domain sizes and grid resolutions, *Muller and Held* [2012] simulated two equilibrium states: with horizontally homogeneous initial conditions over the domain, a convective state which does not aggregate is obtained while an initial bubble of moist humidity surrounded by drier air leads to an aggregated state of convection. The *Khairoutdinov and Emanuel* [2010] simulation also supports the fact that the tropical atmosphere may have these two types of equilibrium states. The relationships between convective aggregation and free-tropospheric humidity along with OLR

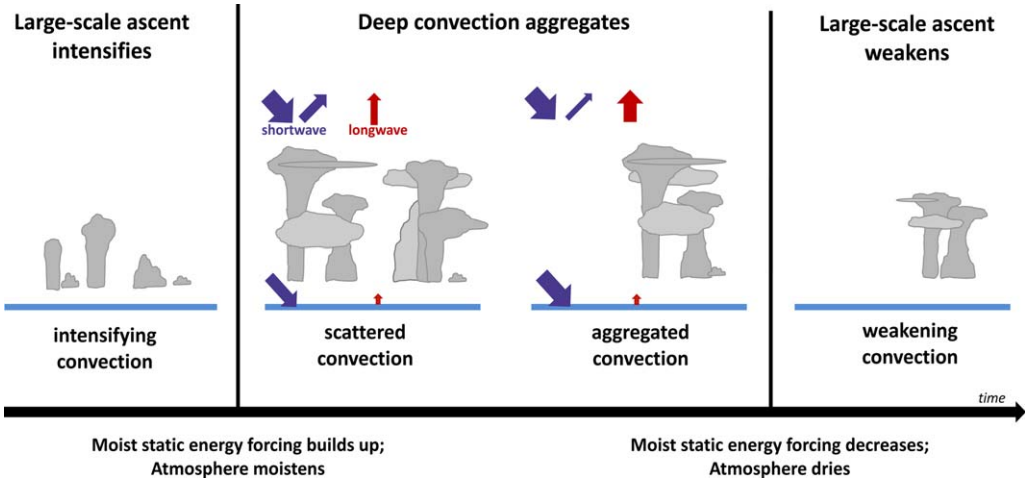

Figure 6. Cartoon summarizing one possible role of convective aggregation in the large-scale ascent regulation, under the assumption that precipitation (or convective intensity) remains unchanged during the aggregation process. From left to right: (1)-(2) Convection develops together with large-scale ascent: Owing to enhanced surface turbulent fluxes and reduced tropospheric radiative cooling resulting from increased moisture and cloudiness in the atmosphere, the net moist static energy flux input into the atmosphere gets stronger. As a result, the large-scale ascent strengthens in order to export moist static energy out of the atmospheric column. (3) Convection aggregates: moisture and cloudiness are reduced, the net moist static energy flux into the atmospheric column decreases, (4) which weakens the large-scale ascent and, in association with a drier free troposphere, weakens convection.

and tropospheric radiative cooling are also found in the studies cited above. Nevertheless, some differences among the studies are to be noted. Regarding the aggregation-related effect on cloudiness and shortwave radiation, this is also found in T12 but is not simulated by CSRM in RCE (see discussion in T12). This seems, however, to be captured by the UK UM at CSRM resolution. In addition, the absence of an aggregation-related effect on turbulent surface fluxes at mesoscale differs notably from the findings at larger scale, where a significant effect was found. Note also that some CSRM studies in RCE showed that aggregation was associated to a warmer atmosphere, which is not found in the present study. A possible explanation for this difference may be the mechanism of temperature homogenization by gravity waves, which operates in nature (and potentially over a large numerical domain) but which is prevented over limited domains such as those used in the CSRM studies in RCE.

4.3. Underlying Mechanisms

[30] The observed relationships between convective aggregation state and the large-scale atmosphere presumably stem from the interplay of a number of processes. The present compositing analysis does not provide any evidence for identifying these underlying mechanisms and understanding the causality of the relationships. We speculate, however, on particular (and nonexclusive) mechanisms.

[31] A two-way interaction between the aggregation state and the large-scale atmospheric state. On the one hand, convective aggregation could first develop from various factors such as statistical fluctuations, spatial heterogeneity (e.g., hysteris in *Muller and Held* [2012]), density currents, etc. Then this aggregated state might lead to a drier atmosphere by reducing the contact area between convective regions and the environment, which results in a reduced mixing between the two regions. Indeed, a larger fraction of convective cells is embedded in moist air, leading to a reduced entrainment of unsaturated environmental air, decreased hydrometeor reevaporation, and thus resulting in an increase of the precipitation efficiency. Thereby, less condensate will be detrained at mid and upper levels, which limits the moistening of the environment, especially at those levels. Furthermore, subsiding environmental parcels are less likely intercepted to mix with moist air from convective regions, which makes the subsidence-induced environmental drying more efficient [*Held et al.*, 1993]. On the other hand, a dry environment would allow for convective development and maintenance only in the aggregated state since this state is likely to reduce the entrainment of dry environmental air entrainment, which would otherwise suppress deep convection. For instance, *Khairoutdinov and Emanuel* [2010] simulated the fact that a dry free troposphere leads convection to be locked in the aggregated state.

[32] A concomittant evolution of the aggregation state and the large-scale atmospheric state. Previous CSRM studies [*Bretherton et al.*, 2005; *Muller and Held*, 2012] suggested an instability mechanism: In the environment, the relatively dry free troposphere leads to a stronger negative vertical gradient in moisture [*Bretherton et al.*, 2005] and/or low-level cloudiness [*Muller and Held*, 2012] at the top of the boundary layer, which allows for strong radiative cooling at this level; a shallow subsidence develops to compensate this radiative cooling; this subsiding motion drives a shallow circulation which exports net moist static energy from dry regions to convective regions, causing moist regions to

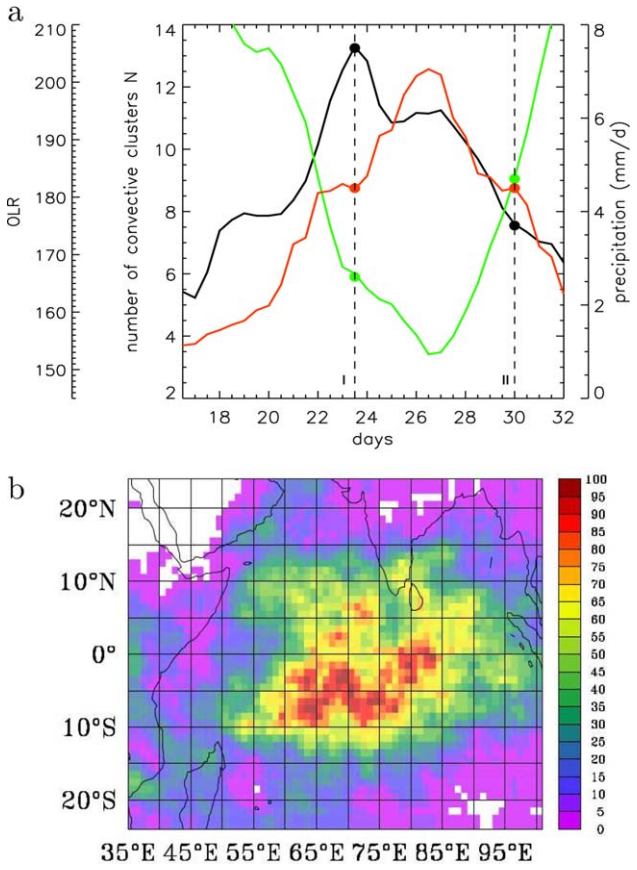

Figure 7. (a) Concurrent evolution of the degree of convection aggregation N (black), precipitation rate (red), and outgoing longwave radiation (OLR; green) during an intraseasonal event in January 1999 over 88°E-94°E/3°N-3°S above the Indian Ocean. (b) Frequency of occurrence of the degrees of aggregation $N > 17$ (i.e., very weak aggregation), calculated for 3° × 3° domains every 1° over the Indian Ocean.

moisten and dry regions to dry further. This circulation is also held partly responsible for the enhancement of turbulent surface fluxes. We may assume that, at mesoscale, such a circulation could not develop as strongly as at larger scale, which could explain the absence of surface flux enhancement with increased aggregation.

[33] Aggregation states and life cycle of convection. The different aggregation states as analyzed in this study could be systematically related to a particular stage of the life cycle of mesoscale convective systems (lasting for 1 to a few days), which could bias the interpretation of the results (i.e., if the nonaggregated state were to correspond to the initial stage of the life cycle while the aggregated state characterized the mature stage of the system). However, an examination of the aggregation state within the few days leading and lagging the time considered in the compositing analysis shows that the aggregation state exhibits a certain persistence (i.e., aggregated states are statistically more aggregated within the few days before and after than nonaggregated states), which is not consistent with the life cycle evolution of a convective system.

4.4. Climatic Implications

[34] In their CSRM simulations, *Khairoutdinov and Emanuel* [2010] found that convective aggregation induced an energy loss for the earth system (surface-atmosphere) owing to enhanced OLR, leading SST to decrease. Although the latter seems in contradiction with the enhanced surface heating by solar radiation, the enhanced tropospheric radiative cooling is supported by our observational study. Under the quasi-equilibrium (QE) assumption, the moist static energy input into the atmosphere (the sum of surface enthalpy fluxes and tropospheric radiative heating) governs the large-scale ascent, and hence convective intensity, for a given gross moist stability [e.g., *Neelin and Held*, 1987; *Raymond et al.*, 2009] (equation (2)).

$$-\omega = \frac{F}{M} \tag{2}$$

where $-\omega$ is a measure of the intensity of the large-scale ascent (or low-level convergence), F is the sum of surface enthalpy fluxes and the tropospheric radiative heating, and M is the gross moist stability as defined by *Neelin and Held* [1987].

[35] According to the present study, under the assumption that the precipitation rate (or convective intensity) does not change on average during the aggregation process, F would decrease with convective aggregation through enhanced tropospheric radiative cooling. Therefore, provided that M is not significantly affected by the aggregation state of convection (which would need to be assessed), convective aggregation is likely to feed back negatively on the large-scale ascent, and hence on convective intensity.

[36] However, on shorter timescales, by reducing interactions between convection and the unsaturated environment, aggregation may favor the mesoscale enhancement of convection, along with mesoscale ascent, at the expense of neighboring regions, where anomalous subsidence may develop. Indeed, previous CSRM studies dealing with the convective aggregation process [e.g. *Bretherton et al.*, 2005] exhibit more consistency with this scenario. Then, if precipitation and mesoscale ascent increase during the aggregation process, the evolution of moisture and tropospheric radiative cooling with aggregation is not straightforward to foresee (on Figures 2 and 4, this corresponds to jumping to different "P colored curves" while moving towards smaller N).

[37] Further analyses are needed to support the above assumptions.

[38] By affecting couplings between convection, radiation, and large-scale ascent and between convection and moisture, convective aggregation may act as a "convective regulating mechanism," as illustrated in Figure 6, and hence is likely to play a role in climatic phenomena. For instance, previous CSRM studies have suggested that convective aggregation is favored above warm SSTs [*Khairoutdinov and Emanuel*, 2010]. The increased radiative cooling of the troposphere together with the enhanced absorption of radiation by the surface, which accompanies convective aggregation, may

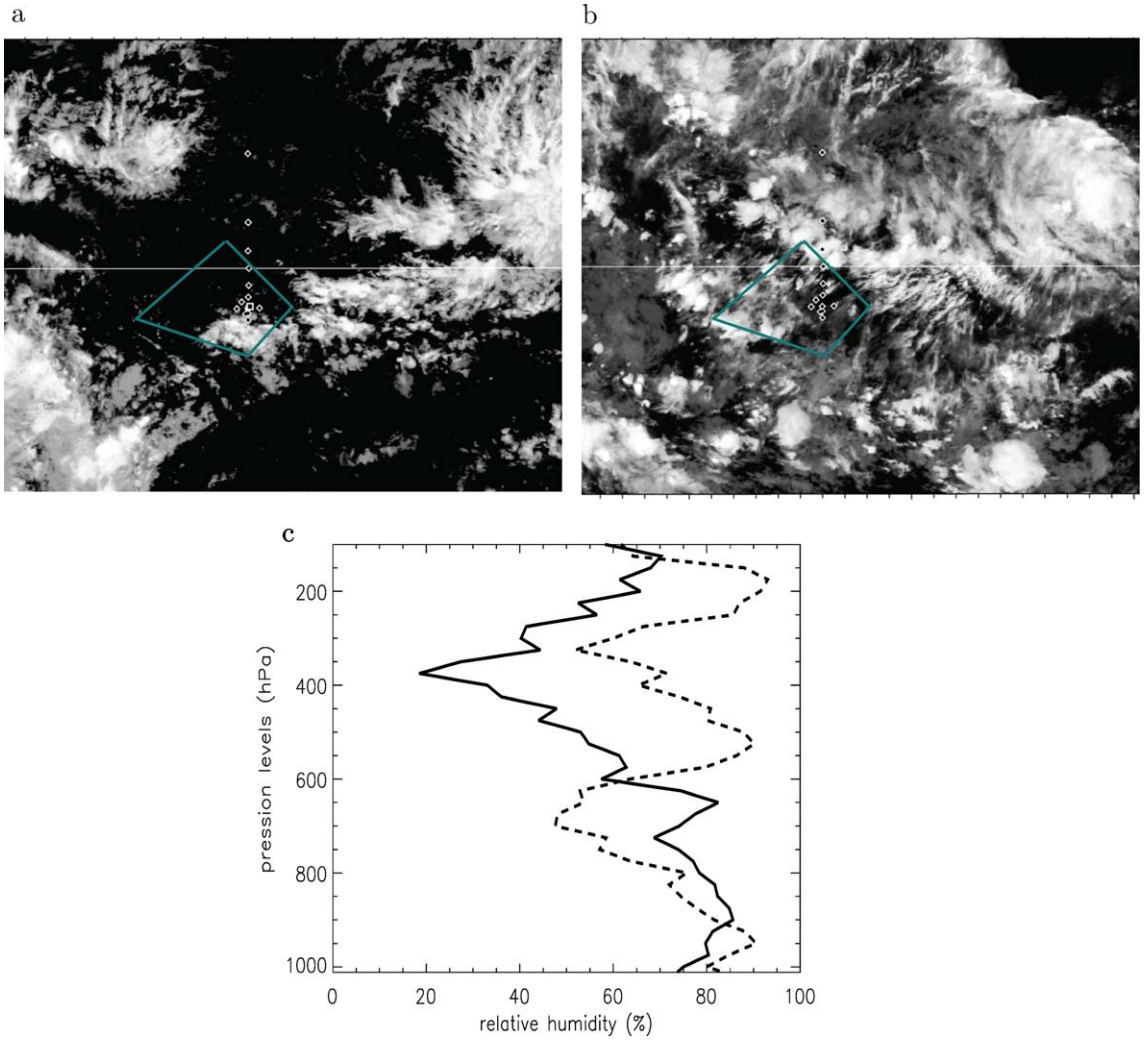

Figure 8. (a) Infrared images from GMS satellite of the 10°N-10°S/145°E-170°E domain on the 10 January 1993 at 00:00 UTC, during the TOGA COARE campaign. The blue lines mark the IFA boundaries. (b) Same as (a) for the 21 January 1993 at 12:00 UTC. Both cases are characterized by an IFA-averaged precipitation rate of about 9 mm/d, IFA-averaged vertical velocities of about −55, −65, −45 hPa d^{-1}, at 800, 500, 300 hPa, respectively, and an IFA-averaged SST of about 29.2°C. (c) Observed IFA-averaged relative humidity profiles for (a) (solid) and (b) (dashed) [*Ciesielski et al.*, 2003].

partly explain the decrease of convective activity above the highest SSTs [*Waliser et al.*, 1993]. This suggestion is consistent with the theory proposed by *Tompkins* [2001], who interprets on the basis of CSRM results the emergence of "hot spots" [e.g., *Waliser*, 1996] as regions where the free troposphere is very dry owing to the self-aggregation of convection in the surroundings. Moisture recovery time allows for SST to warm until convection develops again. Moreover, given that both convection-humidity and convection-radiation couplings are critical in controlling the characteristics of MJO-like phenomena [e.g., *Raymond*, 2001; *Woolnough et al.*, 2001; *Grabowski and Moncrieff*, 2004; *Bony and Emanuel*, 2005], convective aggregation features have the potential to play an active role in such phenomena. For instance, Figure 7a shows a 3 days-lag between the evolution of the number of convective clusters N and that of convective activity during an intraseasonal event over the Indian Ocean. This lag results in asymmetrical increasing and decreasing phases of the convective activity, with regards to the aggregation state: convection in the latter phase is thus more aggregated than in the former one (e.g., the degree of aggregation at time I and II differ by several clusters). Consistently with the relationships found in this study, OLR is stronger in II than in I despite a similar rain rate. This reduced tropospheric diabatic heating associated with aggregation might help the transition toward the decreasing convective phase. Figure 7b shows that nonaggregated convection, which should be associated with positive moisture and diabatic heating anomalies in the troposphere (according to the present study), frequently occurs in the middle of the Indian Ocean, where the active phase of the MJO is known to be triggered. Both examples raise the question of an active role of the aggregation state in

the dynamics of the MJO. We believe that these ideas deserve deeper investigation.

4.5. Implications for Cumulus Parameterizations

[39] Conventional cumulus parameterizations used in climate models assess the amount of convection from the large-scale resolved atmospheric state (humidity, temperature, winds) and the effects of that convection on the large-scale environment. This is made through closures based on moisture convergence [e.g., *Kuo*, 1973; *Tiedtke*, 1989] or quasiequilibrium [e.g., *Arakawa and Schubert*, 1974; *Emanuel*, 1990], among others, and via prescribed parameters governing processes such as entrainment, precipitation efficiency, rain evaporation, or convective cloudiness.

[40] The evaluation and optimization of cumulus parameterizations are often achieved by using single column models (SCM). For this purpose, SCMs are forced with observed large-scale forcings and surface conditions, and the simulated atmospheric properties are compared against those observed (or derived from a CSRM) as averaged over a domain comparable to the model gridbox, such as the Tropical Ocean Global Atmosphere Coupled Ocean Atmosphere Response Experiment (TOGA COARE) intensive fluxes array (IFA) region [e.g., *Emanuel and Živkovic-Rothman*, 1999; *Bechtold et al*., 2000; *Bony and Emanuel*, 2001]. This comparison is generally carried out regardless of the aggregation state of convection. For instance, Figure 8 shows two convective situations observed over the IFA during TOGA COARE. Although both situations are characterized by similar SST and vertical velocities at 300, 500, and 800 hPa, and an equal domain-averaged precipitation rate, they exhibit significant differences in relative humidity and cloudiness: in A, above 600 hPa, the troposphere is drier by 10–20% and midhigh cloud cover is less extended than in B. In view of the statistical relationships highlighted in this study, these differences are consistent with the convective organization contrast between both situations: convection in scene A is aggregated into a unique cluster (Figure 8a) while much more scattered in scene B (Figure 8b). Are conventional convection schemes combined with cloud schemes able to produce different atmospheric states with the same precipitation rate but correspondingly large differences in humidity and cloudiness? Could a particular convective aggregation state be favored in parameterizations owing to their testing against specific cases? In other words, if cumulus parameterizations are tested against well-observed cases of aggregated convection (e.g., scene A), would there be a risk of biasing the modeled precipitation-moisture relationship toward dry conditions, as pointed out by several studies [e.g., *Biasutti et al*., 2006; *Xavier*, 2012]?

[41] Given the number of assumptions and prescribed parameters involved in cumulus parameterizations, the ability of the latter to reproduce observed modulations of convective-radiative and convective-moist couplings associated with the aggregation state of convection is brought into question. The introduction of a prognostic variable "Aggreg(t)," which would constitute an additional degree of freedom describing the aggregation state of convection, might be required. This variable would for instance modulate prescribed characteristics of entrainment, precipitation efficiency, rain evaporation, and/or cloud amount and distribution, in order to relax the strong control of the large-scale on convection and to adjust in turn the effects of the latter on the former. To our knowledge, such an approach has been uniquely adopted by *Mapes and Neale* [2011]. However, efforts consisting in physically representing organizational features [e.g., density currents, *Grandpeix and Lafore*, 2010] may allow for modulations of convective coupling with the large-scale atmosphere.

[42] The mechanisms controlling the evolution of the aggregation state and how the latter modulates the two-way interaction between convection and the large-scale atmospheric state remain to be determined. The ability of the UK Met Office Unified Model at cloud-system-resolving resolutions to reproduce the observed relationships between the aggregation state of convection and the large-scale atmosphere suggests that it will be possible to use this type of model to gain insights into the causal mechanisms underlying these relationships. This constitutes a priority to guide attempts at parameterizing the effects of convective aggregation.

[43] **Acknowledgments.** We wish to thank Thomas Fiolleau for his help in handling Meteosat data. We acknowledge Karim Ramage and Sophie Cloché for their assistance and for providing most datasets used for this study via ClimServ service. We thank Rodrigo Guzman for providing FTH product and for useful discussion about it. This work also benefited from discussions with Jean-Philippe Lafore, Catherine Rio, Nicolas Rochetin, and Laurence Picon. We are grateful to Francoise Guichard and Jean-Luc Redelsperger for providing TOGA COARE GMS images. Comments from two anonymous reviewers helped improving the paper. Cascade simulations were carried out using the UK supercomputer HECToR, which is funded by the Office of Science and Technology through EPSRC's High End Computing Programme. The first author was supported by the European program EMBRACE. C.E. Holloway and S.J. Woolnough were funded by UK NERC grant NE/E00525X/1 and CEH was also funded by UK NERC grant NE/I021012/1.

References

Andersson, A., K. Fennig, C. Klepp, S. Bakan, H. Graßl, and J. Schulz (2010), The Hamburg ocean atmosphere parameters and fluxes from satellite data HOAPS-3, *Earth Syst. Sci. Data*, *2*(2), 215–234, doi:10.5194/essd-2–215-2010.

Arakawa, A. (2004), The cumulus parameterization problem: Past, present, and future, *J. Clim.*, *17*(13), 2493–2525.

Arakawa, A., and W. Schubert (1974), Interaction of a cumulus cloud ensemble with the large-scale environment, part i, *J. Atmos. Sci.*, *31*(3), 674–701.

Aumann, H., et al. (2003), AIRS/AMSU/HSB on the Aqua mission: Design, science objectives, data products, and processing systems, *IEEE Trans. Geosci. Remote Sens.*, *41*, 253–264.

Bechtold, P., et al. (2000), A GCSS model intercomparison for a tropical squall line observed during toga-coare. ii: Intercomparison of single-column models and a cloud-resolving model, *Q. J. R. Meteorol. Soc.*, *126*(564), 865–888.

Biasutti, M., A. Sobel, and Y. Kushnir (2006), AGCM precipitation biases in the tropical Atlantic, *J. Clim.*, *19*, 935–958.

Bony, S., and K. Emanuel (2001), A parameterization of the cloudiness associated with cumulus convection; evaluation using TOGA COARE data, *J. Atmos. Sci.*, *58*(21), 3158–3183.

Bony, S., and K. Emanuel (2005), On the role of moist processes in tropical intraseasonal variability: Cloud-radiation and moisture-convection feedbacks, *J. Atmos. Sci.*, *62*, 2770–2789.

Bretherton, C., P. Blossey, and M. Khairoutdinov (2005), An energy-balance analysis of deep convective self-aggregation above uniform SST, *J. Atmos. Sci.*, *62*, 4273–4292.

Brogniez, H., R. Roca, L. Picon, et al. (2004), Interannual and intraseasonal variabilities of the free tropospheric humidity using meteosat water vapor channel over the tropics, in Eumetsat Meteorological Satellite Conference, 31–4 June, 2004, Prague, Czech Republic.

Brogniez, H., R. Roca, and L. Picon (2006), A clear-sky radiance archive from meteosat "water vapor" observations, *J. Geophys. Res.*, *111*, D21109, doi:10.1029/2006JD007238.

Ciesielski, P., R. Johnson, P. Haertel, and J. Wang (2003), Corrected TOGA COARE sounding humidity data: Impact on diagnosed properties of convection and climate over the warm pool, *J. Clim.*, *16*(14), 2370–2384.

Del Genio, A. (2012), Representing the sensitivity of convective cloud systems to tropospheric humidity in general circulation models, *Surv. Geophys.*, *33*(3), 637–656.

Derbyshire, S., I. Beau, P. Bechtold, J.-Y. Grandpeix, J. Piriou, J.-L. Redelsperger, and P. Soares (2004), Sensitivity of moist convection to environmental humidity, *Q. J. R. Meteorol. Soc.*, *130*, 3055–3079.

Donner, L. (1993), A cumulus parameterization including mass fluxes, vertical momentum dynamics, and mesoscale effects, *J. Atmos Sci.*, *50*(6), 889–906.

Emanuel, K. (1990), A scheme for representing cumulus convection in large-scale models, *J. Atmos. Sci.*, *48*, 2313–2335.

Emanuel, K., and M. Živkovic-Rothman (1999), Development and evaluation of a convection scheme for use in climate models, *J. Atmos. Sci.*, *56*(11), 1766–1782.

Grabowski, W., and M. Moncrieff (2004), Moisture-convection feedback in the tropics, *Q. J. R. Meteorol. Soc.*, *130*, 3081–3104.

Grandpeix, J., and J. Lafore (2010), A density current parameterization coupled with Emanuel's convection scheme. Part I: The models, *J. Atmos. Sci.*, *67*, 881–897.

Held, I., R. Hemler, and V. Ramaswamy (1993), Radiative-convective equilibrium with explicit two-dimensional moist convection, *J. Atmos. Sci.*, *50*, 3909–3909.

Holloway, C., S. Woolnough, and G. Lister (2012), Precipitation distributions for explicit versus parametrized convection in a large-domain high-resolution tropical case study, *Q. J. R. Meteorol. Soc.*, *138*, 1692–1708.

Holloway, C., S. Woolnough, and G. Lister (2013), The effects of explicit versus parameterized convection on the MJO in a large-domain high-resolution tropical case study. Part I: Characterization of large-scale organization and propagation, *J. Atmos. Sc.*, *70*, 1342–1369.

Houze, J. R. (2004), Mesoscale convective systems, *Rev. Geophys.*, *42*, RG4003, doi:10.1029/2004RG000150.

Khairoutdinov, M., and K. Emanuel (2010), Aggregation of convection and the regulation of climate, in Preprints, 29th Conf. on Hurricanes and Tropical Meteorology, p. P2.69, Amer. Meteor. Soc., Tucson, AZ, USA.

Khairoutdinov, M., and D. Randall (2001), A cloud resolving model as a cloud parameterization in the NCAR community climate system model: Preliminary results, *Geophys. Res. Lett.*, *28*(18), 3617–3620.

Kim, D., A. Sobel, E. Maloney, D. Frierson, and I. Kang (2011), A systematic relationship between intraseasonal variability and mean state bias in AGCM simulations, *J. Clim.*, *24*(21), 5506–5520.

Kuo, H. (1973), Further studies of the parameterization of the influence of cumulus convection on large-scale flow, *J. Atmos. Sci.*, *31*, 1232–1240.

Laing, A., and M. Fritsch (1997), The global population of mesoscale convective complexes, *Q. J. R. Meteorol. Soc.*, *123*, 389–405.

Liebmann, B., and C. Smith (1996), Description of a complete (interpolated) OLR dataset, *Bull. Am. Meteorol. Soc*, *77*, 1275–1277.

Lin, J., et al. (2006), Tropical intraseasonal variability in 14 IPCC AR4 climate models. Part I: Convective signals, *J. Clim.*, *19*, 2665–2690.

Mapes, B., and R. Neale (2011), Parameterizing convective organization to escape the entrainment dilemma, *J. Adv. Model. Earth Syst*, *3*, M06004, doi:10.1029/2011MS000042.

Moncrieff, M., and E. Klinker (1997), Organized convective systems in the tropical western pacific as a process in general circulation models: A TOGA COARE case-study, *Q. J. R. Meteorol. Soc.*, *123*(540), 805–827.

Muller, C., and I. Held (2012), Detailed investigation of the self-aggregation of convection in cloud-resolving simulations, *J. Atmos. Sci.*, *69*(8), 2551–2565.

Neelin, J., and I. Held (1987), Modeling tropical convergence based on the moist static energy budget, *Mon. Weather Rev.*, *115*(1), 3–12.

Raymond, D. (2001), A new model of the Madden-Julian oscillation, *J. Atmo Sci.*, *58*(18), 2807–2819.

Raymond, D., S. Sessions, A. Sobel, and Z. Fuchs (2009), The mechanics of gross moist stability, *J. Adv. Model. Earth Syst*, *1*, 9, doi:10.3894/JAMES.2009.1.9.

Redelsperger, J.-L. (1997), The mesoscale organization of deep convection, in *The Physics and Parameterization of Moist Atmospheric Convection*, edited by R. K. Smith, pp. 59–98, Kluwer Acad.

Rio, C., F. Hourdin, J. Grandpeix, and J. Lafore (2009), Shifting the diurnal cycle of parameterized deep convection over land, *Geophys. Res. Lett.*, *36*, L07809, doi:10.1029/2008GL036779.

Roca, R., M. Viollier, L. Picon, and M. Desbois (2002), A multisatellite analysis of deep convection and its moist environment over the Indian ocean during the winter monsoon, *J. Geophys. Res.*, *107*(D19), 8012,doi:10.1029/2000JD000040.

Rossow, W., and R. Schiffer (1999), Advances in understanding clouds from ISCCP, *Bull. Am. Meteorol. Soc.*, *80*, 2261–2288.

Sanderson, B., K. Shell, and W. Ingram (2010), Climate feedbacks determined using radiative kernels in a multi-thousand member ensemble of AOGCMs, *Clim. Dyn.*, *35*(7), 1219–1236.

Simmons, A. J., S. Uppala, D. Dee, and S. Kobayashi (2007), ERA-Interim: New ECMWF reanalysis products from 1989 onwards., ECMWF Newsletter No., 110.

Stephens, G., T. L'Ecuyer, R. Forbes, A. Gettlemen, J. Golaz, A. Bodas-Salcedo, K. Suzuki, P. Gabriel, and J. Haynes (2010), Dreary state of precipitation in global models, *J. Geophys. Res.*, *115*, D24211, doi:10.1029/2010JD014532.

Susskind, J., C. Barnet, and J. Blaisdell (2003), Retrieval of atmospheric and surface parameters from airs/AMSU/HSB data in the presence of clouds, *IEEE Trans. Geosci. Remote Sens.*, *41*(2), 390–409.

Thayer-Calder, K., and D. Randall (2009), The role of convective moistening in the Madden-Julian oscillation, *J. Atmos. Sci.*, *66*(11), 3297–3312.

Tiedtke, M. (1989), A comprehensive mass flux scheme for cumulus parameterization in large-scale models, *Mon. Weather Rev.*, *117*(8), 1779–1800.

Tobin, I., S. Bony, and R. Roca (2012), Observational evidence for relationships between the degree of aggregation of deep convection, water vapor, surface fluxes and radiation, *J. Clim.*, *25*(20), 6885–6904.

Tompkins, A. (2001), On the relationship between tropical convection and sea surface temperature, *J. Clim.*, *14*(5), 633–637.

Waliser, D. (1996), Formation and limiting mechanisms for very high sea surface temperature: Linking the dynamics and the thermodynamics, *J. Clim.*, *9*(1), 161–188.

Waliser, D., N. Graham, and C. Gautier (1993), Comparison of the highly reflective cloud and outgoing longwave radiation datasets for use in estimating tropical deep convection., *J. Clim.*, *6*, 331–353.

Woolnough, S., J. Slingo, and B. Hoskins (2001), The organization of tropical convection by intraseasonal sea surface temperature anomalies, *Q. J. R. Meteorol. Soc.*, *127*(573), 887–907.

Wu, X., and M. Moncrieff (1996), Collective effects of organized convection and their approximation in general circulation models, *J. Atmos. Sci.*, *53*(10), 1477–1495.

Xavier, P. (2012), Intraseasonal convective moistening in cmip3 models, *J. Clim.*, *25*(8), 2569–2577.

Zhang, Y., W. Rossow, A. Lacis, V. Oinas, and M. Mishchenko (2004), Calculation of radiative fluxes from the surface to top of atmosphere based on ISCCP and other global data sets: Refinements of the radiative transfer model and the input data, *J. Geophys. Res.*, *109*, D19105, doi:10.1029/2003JD004457.

Zhu, H., H. Hendon, and C. Jakob (2009), Convection in a parameterized and superparameterized model and its role in the representation of the MJO, *J. Atmos. Sci.*, *66*(9), 2796–2811.